

High-performance EUV/soft X-ray ellipsometry system using multilayer mirrors

Tomoaki Kawamura,^{a*} Jean-Jacques Delaunay,^b Hisataka Takenaka,^c Takayoshi Hayashi^b and Yoshio Watanabe^a

^aNTT Basic Research Laboratories, 3-1 Morinosato, Wakamiya, Atsugi, Kanagawa 243-01, Japan, ^bNTT Integrated Information and Energy System Laboratories, 3-9-11 Midoricho, Musashino, Tokyo 180, Japan, and ^cNTT Advanced Technology Corporation, 3-9-11 Midoricho, Musashino, Tokyo 180, Japan.

E-mail: kawamura@will.brl.ntt.co.jp

(Received 4 August 1997; accepted 3 November 1997)

A high-performance EUV/soft X-ray ellipsometry system using multilayer mirrors has been developed. A couple of multilayer mirrors were used for the polarizer, and two multilayer mirrors were used for the rotating analyser. The multilayer mirrors were optimized to obtain a medium extinction of about 2000. An extinction ratio of the polarizer up to 10^4 can be achieved by using two multilayer mirrors, and the calculated reflectivity was more than 35%. The calculated error of the optical elements reveals that the error of the polarizer and misalignment optical parts is mainly of the first order, and that of the analyser is of the second order.

Keywords: ellipsometry; EUV; soft X-rays; polarization; multilayers; extinction.

1. Introduction

Ellipsometry has been applied to determine the thickness and optical constants of thin layers. Recently, spectroscopic ellipsometry has been introduced and applied for *in situ* monitoring processes (Aspnes, 1981). This method is also used for determining the optical constants of ultra-thin layers (Archer, 1962), analysing the structure of adsorbed atoms on a clean surface (Hanekamp *et al.*, 1982), and investigating the growth mechanism of III–V semiconductors (Maracas *et al.*, 1995).

Recently, owing to the development of light sources and optical elements (Kimura *et al.*, 1990), Yamamoto *et al.* (1996) demonstrated the possibility of ellipsometry in the EUV/soft X-ray region by analysing the metal–silicon interface. The advantages of using EUV and soft X-rays are as follows. (i) The lower detection limit of film thickness is increased; ordinary visible ellipsometry is not effective for the thin films of less than 1 nm thickness because of the long wavelength. (ii) The interaction mechanism between EUV/soft X-rays and materials is simpler due to the inner-shell activation. This feature makes it easy to interpret the experimental result.

Recent developments in multilayer fabrication processes have made available good reflectors in the EUV/soft X-ray region. By using Mo/Si multilayer mirrors, one can easily obtain high-reflectance mirrors, up to 60% with normal inci-

dence at 13 nm (Takenaka *et al.*, 1995). If they are used at 45° of the incident angle, they work as good polarizers with a high reflectivity of 80%. The reflectivity ratio of the *p* component to the *s* component of these mirrors is 10^2 – 10^3 , which is still lower than that of visible polarizers (10^5). Furthermore, the errors due to the imperfections of the optical elements are still unknown.

In this report we discuss the practical requirements for applying the EUV/soft X-ray ellipsometry to the semiconductor materials, and present the design of the new ellipsometry system, with high extinction ratio achieved by using multilayer mirrors. Additionally, we describe the multilayer design for X-ray ellipsometry, and present the theoretical performance.

2. Errors due to imperfections of polarizer/analyser

The principle of EUV/soft X-ray ellipsometry is the same as that of visible ellipsometry. The change in the polarization state of the reflected beam is expressed in the form of complex reflection coefficients for the polarized beams parallel (R_p) and perpendicular (R_s) to the plane of incidence,

$$R_p/R_s \{ \equiv |R_p|/|R_s| \exp[i(\delta_p - \delta_s)] \} = \tan \Psi \exp(i\Delta), \quad (1)$$

where $\tan \Psi \{ \equiv |R_p|/|R_s| \}$ and $\Delta \{ \equiv \delta_p - \delta_s \}$ are the amplitude change and phase difference between the *p* and *s* components, respectively.

Fig. 1 shows the relative changes of $(\Delta - \Psi)$ in Si/Si_{1-x}Ge_x/Si structures by varying the Ge ratio from 0.0 to 0.8 and the thickness of the Si_{1-x}Ge_x layer from 0.0 to 5.0 nm. The incident angle is set at 50° from the surface normal, which is near the Brewster angle of EUV/soft X-rays. Results from calculations show that a large difference in Δ is observed for the increase of the Si_{1-x}Ge_x layer thickness. The resolutions of the thickness and stoichiometry are estimated at less than 0.1 nm and 20%, respectively. The upper limit of the thickness is considered to be about 10 nm due to the short wavelength of EUV/soft X-rays.

Since the fabrication of the $\lambda/4$ phase shifter in the EUV/soft X-ray region is difficult, the rotating analyser/polarizer method is usually used for measuring the ellipsometric parameters. To evaluate the ellipsometry errors we used Jones matrices (Azzam & Bashara, 1971) for the polarizer–sample–analyser system as follows,

$$M = R(-\theta) A R(\theta) S R(\varphi) P, \quad (2)$$

$$R(\theta) = \begin{pmatrix} \cos \theta & -\sin \theta \\ \sin \theta & \cos \theta \end{pmatrix}, \quad A = \begin{pmatrix} 1 & 0 \\ 0 & \gamma_A \end{pmatrix},$$

$$S = \begin{pmatrix} R_s & 0 \\ 0 & R_p \end{pmatrix}, \quad P = \begin{pmatrix} 1 & 0 \\ 0 & \gamma_P \end{pmatrix},$$

$$\gamma_A = |\gamma_A| \exp(i\delta_A), \quad \gamma_P = |\gamma_P| \exp(i\delta_P).$$

Here, M is the Jones matrix for all systems, and A , S and P represent the matrices for the analyser, sample and polarizer elements, respectively. The considered errors are the complex amplitude ratio, γ_P , γ_A . φ and θ represents the azimuth angles for the polarizer and the analyser.

First we consider the errors of the polarizer/analyser system without samples ($R_s = R_p = 0$, $\varphi = \pi/4$). Based on (2), one can derive the observed intensity $I(\theta)$ by including the first- and

second-order errors,

$$I(\theta) (\equiv E_x/E_y) \simeq 1 + \sin 2\theta + 2|\gamma_p| \cos 2\theta \cos \delta_p + (|\gamma_A|^2 + |\gamma_p|^2)(1 - \sin 2\theta). \quad (3)$$

It should be noted that the errors from the polarizer and analyser are not equivalent as shown in (3). The errors derived from the polarizer are of the first order, since the errors of the analyser are of the second order (Azzam & Bashara, 1971).

Next we treat the more complicated system including the samples. For the ellipsometry measurement, absolute intensity is not important; hence, we can write the sample reflectivity as

$$R_s = \cos \alpha \exp(-i\delta/2),$$

$$R_p = \sin \alpha \exp(i\delta/2),$$

$$R_p/R_s = \tan \alpha \exp(i\delta).$$

By using $\varphi = \pi/4$, the observed intensity with rotating angle θ can be expressed as

$$I(\theta) \simeq 1 + \cos 2\theta \cos 2\alpha + \sin 2\theta \sin 2\alpha \cos \delta + A|\gamma_p| + B(|\gamma_A|^2 + |\gamma_p|^2), \quad (4)$$

where

$$A = 2(\cos 2\theta + \cos 2\alpha) \cos \delta_p - \sin 2\alpha \sin 2\theta \sin \delta \sin \delta_p,$$

$$B = 1 - \cos 2\theta \cos 2\alpha - \sin 2\theta \sin 2\alpha \cos \delta.$$

These results show that the requirement for polarizers is more severe than that for analysers. When an extinction $|\gamma_p|^2$ up to 10^{-4} is required for polarizers, we can use the lower extinction components of about 10^{-2} for the analysers.

3. Instrument

3.1. Design of polarizer/analyser

According to the small difference of refractive indices, a realistic geometry for generating linear polarization is one using multilayer mirrors at about 45° (Dhez, 1987). Owing to the amplitude enhancement due to the interference effect, the multilayer polarizer has both wavelength and angle selectivities.

The parameters for the multilayer mirrors we used are the types of low and high-Z elements, thickness, the ratio of layers, the incident angle, the wavelength and the number of periods.

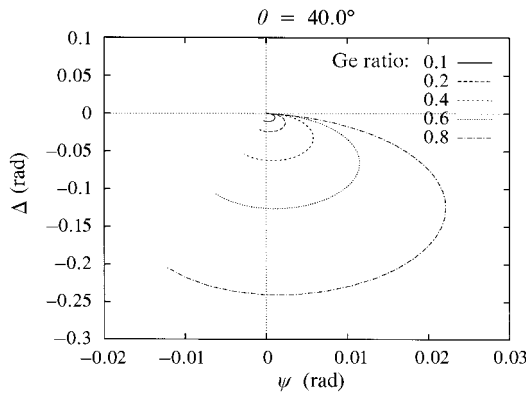


Figure 1
(Ψ - Δ) traces of $\text{Si}/\text{Si}_{1-x}\text{Ge}_x/\text{Si}$ structures.

Table 1

Multilayer mirror parameters for type 1 and type 2 mirrors.

	$P (I_p/I_s)$	I_s	λ (nm)	θ ($^\circ$)	d (nm)	γ	N_p
Type 1	2000	60%	14.00	47.6	9.8	0.2	20
Type 2	1×10^5	80%	12.95	47.0	9.0	0.38	30

increase the reflectivity, low absorption for each layer and a high refractive index for the high-Z layer are required. With respect to this, silicon is the best candidate for the low-Z material. Molybdenum, ruthenium, aluminium and barium are possible candidates for the high-Z layers. Considering the ease of fabrication, Mo/Si was selected as a suitable combination for our purpose.

For designing multilayer mirrors, the recursive method is used with fixed wavelength. Table 1 shows the final structural parameters that we selected for two polarizers with middle and high performance.

Figs. 2 and 3 show the reflectivity of the s component and the extinction ratio I_p/I_s of s and p components by taking the resolution of the incident beam into account. Roughly, an extinction ratio of more than 2000 is obtained with wavelengths from 13.5 to 14.5 nm for the type 1 mirror. There is little decrease in the extinction ratio of the type 1 mirror when the incident wavelength resolution is reduced to 70. In spite of the high extinction ratio, up to 10^5 for the type 2 mirror, the degradation of the extinction is large, with decreasing wavelength resolution. Additionally, the reflected beam intensity of the type 2 mirror changes remarkably with varying wavelength. This feature decreases the optical margin and throughput, and the need to pin-point alignment for obtaining the extinction ratio and intensity.

Similar results were obtained when the angle divergence of the incident beams was changed. Additionally, the defects of multilayer mirrors, such as interface roughnesses, density variation, the error of the layer periods, and the thickness ratio of the two layers, also cause unexpected fluctuations in the extinction ratio and intensity of the type 2 mirror. Considering these factors, it is better to use a set of type 1 mirrors for the polarizer to obtain a

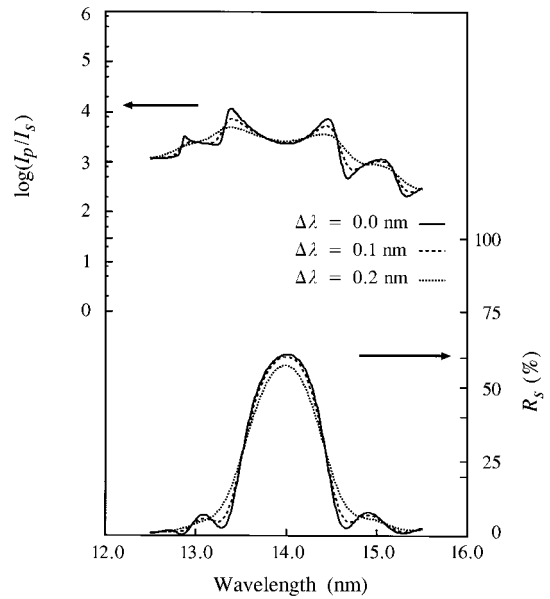


Figure 2
Extinction ratio and reflectivity of the type 1 mirror.

high extinction ratio of up to 10^6 . The throughput is estimated to be about 35% when using two mirrors, and 20% by addition of the analysing mirror.

3.2. Mechanical design

A set of multilayer mirrors was installed on the inclined plate at 45° for generating a linear polarized 45° beam. The sample stage and the analysing mirrors were set in the same vacuum chamber, and the incident angle to the sample and the scattering angle from the sample were varied independently. The sample and the analyser stage were rotated by the rotation stage set in the air through the magnetic feedthrough. The mechanical resolution for the sample was 0.002° , and that for the analyser was 0.005° , which are sufficient for measuring the polarization. The analyser mirror and the detector are set on the stage, which

can rotate by 360° around the beam path. An X-ray PIN diode and microchannel plate (MCP) were used for detecting EUV and X-rays coming from the sample.

4. Summary

We have developed a high-performance EUV/X-ray ellipsometry system. Simulation of the $\text{Si}/\text{Si}_{1-x}\text{Ge}_x/\text{Si}$ structures reveals that a higher extinction ratio, up to 10^4 , is required for the polarizer, while 10^2 is high enough for the analyser. Two kinds of multilayer mirrors for the polarizer and analyser were designed; one had a medium extinction of about 2000, and the other 1×10^5 . The extinction and reflectivity calculations including the experimental errors showed that a set of multilayer mirrors with medium extinction is superior to one high-extinction mirror for a linear polarizer.

Calculation results were used to develop a polarizer-sample-analyser ellipsometry system. A set of mirrors was installed on the inclined plate at 45° for generating the linear polarized beam. Two multilayer mirrors were set on the analyser stage, which rotates 360° around the beam axes. The estimated throughput using Mo/Si multilayer mirrors without samples was about 20%.

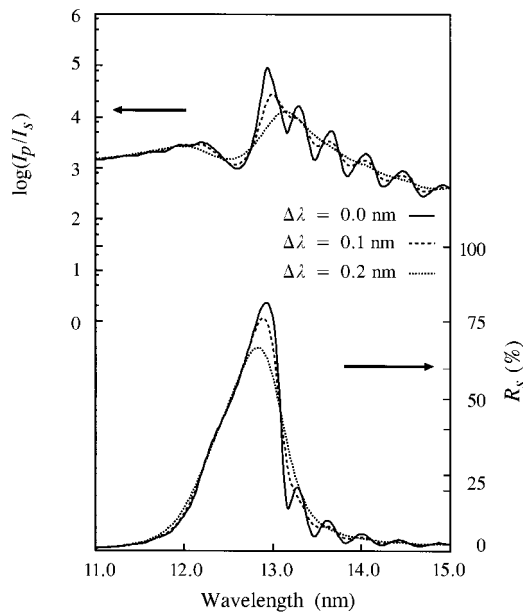


Figure 3
Extinction ratio and reflectivity of the type 2 mirror.

References

- Archer, R. J. (1962). *J. Opt. Soc. Am.* **52**, 970–977.
- Aspnes, D. E. (1981). *SPIE*, **276**, 188–195.
- Azzam, R. M. A. & Bashara, N. M. (1971). *J. Opt. Soc. Am.* **61**, 600–607.
- Dhez, P. (1987). *Nucl. Instrum. Methods*, **A261**, 66–71.
- Hanekamp, L. J., Lisowski, W. & Boatsma, G. A. (1982). *Surf. Sci.* **118**, 1–18.
- Kimura, H., Yamamoto, M., Yanagihara, M., Maehara, T. & Namioka, T. (1990). *Rev. Sci. Instrum.* **63**, 1379–1382.
- Maracas, G. N., Kuo, C. H., Anand, S., Droopad, R., Sohie, G. R. L. & Levola, T. (1995). *J. Vac. Sci. Technol.* **A13**, 727–732.
- Takenaka, H., Kawamura, T., Ishii, Y. & Asagiri, S. (1995). *J. Appl. Phys.* **78**, 5227–5230.
- Yamamoto, M., Mayama, K., Kimura, H., Goto, Y. & Yanagihara, M. (1996). *J. Electron Spectrosc. Relat. Phenom.* **80**, 465–468.